Advanced Healthcare Materials

Photopolymerizable platelet lysates hydrogels for customizable 3D cell culture platforms

--Manuscript Draft--

Manuscript Number:	adhm.201800849R1
Full Title:	Photopolymerizable platelet lysates hydrogels for customizable 3D cell culture platforms
Article Type:	Full Paper
Section/Category:	
Keywords:	hydrogels platelets personalized medicine tissue engineering human extracellular matrix
Corresponding Author:	Catarina de Almeida Custódio Universidade de Aveiro CICECO Aveiro, --None-- PORTUGAL
Additional Information:	
Question	**Response**
Please submit a plain text version of your cover letter here.	Dear Editor, We submit now the revised version of our manuscript attending to the comments of the referees. We thank both of them for their constructive input and hope that they are satisfied with the answers and changes in the manuscript. We look forward to a positive reply With best regards Catarina Custódio
Do you or any of your co-authors have a conflict of interest to declare?	No. The authors declare no conflict of interest.
Corresponding Author Secondary Information:	
Corresponding Author's Institution:	Universidade de Aveiro CICECO
Corresponding Author's Secondary Institution:	
First Author:	Sara Santos
First Author Secondary Information:	
Order of Authors:	Sara Santos
	Catarina de Almeida Custódio
	João Mano
Order of Authors Secondary Information:	
Abstract:	3D cell cultures have emerged as a setting that resembles in vivo environments replacing the traditional 2D. Over the recent years an extensive effort has been made on the development of more physiologically relevant 3D cell culture platforms. Extracellular matrix based materials have been reported as a bioactive and biocompatible support for cell culture. For example, human plasma derivatives have been extensively used as cell culture platforms. Despite all the promising results, in most cases this type of materials have poor mechanical properties and stability in vitro. Here we propose plasma based hydrogels with tunable mechanical properties and increased stability. Platelet lysates were modified by addition of methacryloyl groups

	(PLMA) that polymerizes in controlled geometries upon UV-light exposure. The hydrogels could also generate porous scaffolds after lyophilization. Our results showed that PLMA materials own increased mechanical properties that can be adjustable by changing PLMA concentration or modification degree. Cells readily adhere, proliferate and migrate, exhibiting high viability when encapsulated in PLMA hydrogels. The innovation potential of PLMA materials is based on the fact that is a complete xeno-free solution for human cell culture, thus an effective alternative to the current gold standards for 3D cell culture based on animal products.

WILEY-VCH

DOI: 10.1002/ ((please add manuscript number))
Article type: Full Paper

Title Photopolymerizable platelet lysates hydrogels for customizable 3D cell culture platforms

*Author(s), and Corresponding Author(s)** *Sara C. Santos[1], Catarina A. Custódio[1]*, João F. Mano[1]**

((Optional Dedication))

1- Department of Chemistry, CICECO, University of Aveiro, Campus Universitário de Santiago, 3810-193 Aveiro, Portugal

E-mail: catarinacustodio@ua.pt and jmano@ua.pt

Keywords: (hydrogels, platelets, personalized medicine, tissue engineering, human extracellular matrix)

Three-dimensional (3D) cell culture platforms have emerged as a setting that resembles *in vivo* environments replacing the traditional 2-D cell culture systems. Over the recent years an extensive effort has been made on the development of more physiologically relevant 3D cell culture platforms.

Extracellular matrix (ECM) based materials have been reported as a bioactive and biocompatible support for cell culture. For example, human plasma derivatives have been extensively used as cell culture platforms. Despite all the promising results, in most cases this type of materials have poor mechanical properties and poor stability *in vitro*. Here we propose plasma based hydrogels with tunable mechanical properties and increased stability. Platelet lysates were modified by addition of methacryloyl groups (PLMA) that polymerizes in controlled geometries upon UV light exposure. The hydrogels could also generate porous scaffolds after lyophilization. Our results showed that PLMA materials own increased mechanical properties that can be easily adjustable by changing PLMA concentration or modification degree. Cells readily adhere, proliferate and migrate, exhibiting high viability when encapsulated in PLMA hydrogels.

The innovation potential of PLMA materials is based on the fact that is a complete xeno-free solution for human cell culture, thus an effective alternative to the current gold standards for 3D cell culture based on animal products.

1.Introduction

Culturing cells in two-dimensional (2D) substrates is still widely used for *in vitro* cell based assays. However, 2D platforms do not replicate the complex and dynamic *in vivo* cell microenvironment.[1,2] Three-dimensional (3D) cell culture systems have gained interest as they can better mimic the native extracellular matrix (ECM), its mechanical and biochemical signals and *in vivo* cell growth.[1–3] The 3D cell culture platforms have been applied in drug discovery, cancer cell biology, stem cell study, engineered functional tissues for implantation and other cell-based therapies.[2,4]

In these shift from 2D to 3D cell culture, hydrogels have been emerging as one of the most promising 3D platforms. Hydrogels are soft 3D insoluble hydrophilic network systems with high water content, that allow for an easy transport of oxygen, nutrients and cell metabolites. Due to its similarities to the native ECM, both structural and compositional level, hydrogels have been adopted for 3D culture applications as they better mimic the physiological human context.[3,5–7]

Currently, the gold standards for 3D cell culture for several cell types are collagen and the basement membrane proteins derived from the Engelbreth-Holm-Swarm (EHS) tumor.[8,9] Both matrices have shown to drive cellular self-organization and complex morphogenetic processes that resulted into sophisticated platforms for cell culture.[10] However, cell culture strategies using this type of materials goes against current animal-free approaches. Moreover, the mixture of proteins derived from the EHS tumor is a viscous material that quickly gelifies into very soft matrices, making it difficult to handle. As an alternative to animal-based gels, synthetic polymer-based gels have also been proposed to recreate native cell

microenvironments.[8] Despite the design flexibility for specific applications, such synthetic systems are typically expensive and their synthesis can be time consuming, requiring often multiple steps. Currently, striving toward personalized medicine and targeted therapy, creating the most appropriate material that closely mimics the *in vivo* microenvironment is one of the most important topics to address.

Platelet concentrates (PC), obtained from whole blood by a differential centrifugation process, are an important source of growth factors (GFs), cytokines and other proteins.[11–13] Platelet lysates (PL) are derivatives obtained from PC by freeze/thaw cycles.[14,15] Previous works have reported the potential of PC based materials for cell culture.[16–18] Moreover, PC and PL have been used as an autologous material containing bioactive molecules, locally enhancing wound healing[19–21], bone growth and cartilage repair[22–25] and tissue healing[26]. Platelet-rich plasma (PRP) and PL based hydrogels have also been explored as 3D cell culture platforms and for tissue engineering (TE). Despite their great potential, a major disadvantage of these hydrogels is their poor mechanical properties and poor stability *in vitro* which hinders its application. The main goal in this study was the development of PL based hydrogels with increased mechanical properties and improved stability. Here we proposed the modification of PL by chemical conjugation with a photoresponsive group in order to achieve PL-based photopolymerizable materials with finely tunable mechanical properties. Such PL derived materials should provide a functional support for cell growth and interact with cells to control their function, guiding the process of tissue morphogenesis.

We hypothesize that the herein proposed blood-derived materials that could have an allogenic origin, could be adequate to produce customized robust matrices rich in bioactive factors to be used as general platform for 3D cell cultures and in TE strategies in a more physiological setting.

2.Experimental Section

2.1.Synthesis of methacryloyl platelet lysates (PLMA)

PLMA were synthesized by reaction with methacrylic anhydride 94% (MA) (Sigma-Aldrich, Germany). PL (STEMCELL Technologies, Canada) were thawed at 37ºC and to 10ml (total protein content 6.3g/dL) of this solution, either 100 or 300µL of MA was added, in order to synthesize PLMA100 (low modification degree) or PLMA300 (high modification degree) respectively. The reaction was performed under constant stirring at room temperature. The synthesized PLMA was then purified by dialysis with Float-A-Lyzer G2 Dialysis Device 3.5-5 kDa (Spectrum, USA) against deionized water during 24h to remove the excess of MA. The PLMA solution was filtered with a 0.2 µm filter in order to sterilize it, frozen with liquid nitrogen, lyophilized and stored at 4ºC until further use.

2.2.PLMA characterization

2.2.1.^{1}H NMR

NMR analysis was used to verify the effective functionalization of original PL. Solutions of 10 mg/mL of non-modified PL and PLMA in methyl sulfoxide-d6 (DMSO) 99.5% (Fisher Scientific, USA) were prepared and analyzed by ^{1}H-NMR with 18 seconds relaxation delay and 300 scans. The ^{1}H NMR spectra were recorded on a Bruker AMX 300 spectrometer at 300.13 MHz.

2.2.2.In-gel digestion and mass spectrometry analysis

PL, PLMA100 and PLMA300 were separated in a 4–12% (w/v) acrylamide NuPAGE gradient pre-cast gel (LifeTechnologies) and extracted gel fractions were subjected to in-gel tryptic digestion. Protein bands were distained with 50% (v/v) acetonitrile, reduced with 10 mM DTT, alkylated with iodoacetamide 55 mM and digested overnight at 37 °C with 6.7 ng/mL

trypsin. Digested peptides extraction was performed in a water bath sonifier with alternate 100% acetonitrile and 5% formic acid incubations. Analysis of digested peptides was performed on an ekspert™ NanoLC 425 cHiPLC® coupled to a TripleTOF 6600 with a NanoSpray® III ion source (Sciex). Reversed-phase separation was performed in a trap-elute mode using a ChromXP C18 column (75 µm x 15 cm, 3 µm, 120 Å, Sciex) and a ChromXP C18 trap column (200 µm x 0.5 mm, 3 µm, 120 Å, Sciex). The flow-rate was 300nl/min and the gradient was as follows: 0-1 min, 95% A (0.1% formic acid in water, fisher); 1-91 min, 5-30% B (0.1% formic acid in acetonitrile, fisher); 91-93 min, 30-80% B; 93-108 min, 80% B; 108-110 min, 80-5% B; 110-127 min, 5% B. Electrospray was achieved using an uncoated fused-silica PicoTip™ emitter (360 µm O.D., 20 µm I.D., 10 ± 1.0 µm tip I.D., New Objective, Oullins, France), with the following source parameters: 15 GS1, 0 GS2, 30 CUR, 2.4 keV ISVF and 100 °C IHT. An information dependent acquisition (IDA) method was set with a TOF-MS survey scan of 400-2000 m/z. The 50 most intense precursors were selected for subsequent fragmentation and the MS/MS were acquired in high sensitivity mode.

The spectra were processed and analyzed using ProteinPilot™ software, with the Paragon search engine (version 5.0, Sciex). The data dictionary and the parameter translation files were modified to incorporate the methacrylic anhydride modification in primary amines (5% probability), with preference for lysine residues (49% probability). A database was retrieved from UniProt (Swissprot, March 2017 version) and a *Homo sapiens* restriction was used. TripleTOF 6600 was selected as the Instrument used and Gel-based ID as a special factor. The ID focus was on biological modifications and Amino acid substitutions. The search effort was set as thorough and an FDR analysis was performed. Only the proteins with Unused Protein Score above 1.3 and 95% confidence were considered.

2.3.Hydrogel formation

Lyophilized PLMA was dissolved in a solution of 0.5% (w/v) 2-hydroxy-4'-(2-hydroxyethoxy)-2-methylpropiophenone (Sigma-Aldrich, Germany) in PBS (Thermo Fischer Scientific, USA) to final concentrations of 10%, 15% or 20% (w/v) of PLMA. Hydrogels were made by pipetting the polymer solution to polydimethylsiloxane (PDMS) (Dow Corning, USA) molds with 3.5mm or 6mm diameter followed by UV irradiation (0.95 W/cm^2) during 60s.

2.4.PLMA hydrogels characterization

2.4.1.Structural properties of PLMA hydrogels by Scanning Electron Microscopy

The hydrogels were frozen with liquid nitrogen and then lyophilized. Samples were sputter-coated with gold and imaged via SEM using Ultra-high Resolution Analytical Scanning Electron Microscope HR-FESEM Hitachi SU-70 (Hitachi, Tokyo, Japan). SEM images were analyzed by ImageJ software for pore size measurement.

2.4.2.Water content

Hydrogel samples of PLMA100 and PLMA300 at 10%, 15% and 20% (w/v) were made in triplicate and immersed in 5 mL of PBS. Samples were incubated at room temperature during 16 hours. After incubation the wet weight (w_w) was measured and samples were frozen and lyophilized. After lyophilization, dry weight (w_d) was measured and compared with the initial wet weight. The water content was calculated according to the following equation:

$$\text{Water content (\%)} = \frac{w_w - w_d}{w_w} \times 100 \qquad (1)$$

2.4.3.Mechanical properties

The mechanical behavior of PLMA hydrogels was characterized on the basis of compression tests employing a Universal Mechanical Testing Machine Shimadzu MMT-101N (Shimadzu Scientific Instruments, Kyoto, Japan) equipped with a load cell of 100 N. To this

end, both unidirectional and cyclic compression assays were performed at room temperature on fresh-prepared cylindrical hydrogels specimens with a diameter of 3.5 mm and height of 2 mm. The nominal stress was obtained by dividing the compressive load by the initial (uncompressed) cross-sectional area of the specimen. The compressive modulus was defined as the slope of the linear region of the strain/stress curve, corresponding to 0–10% strain. Ultimate stress and ultimate strain values were taken as the point where failure of the hydrogel occurred.

2.4.4.Rheological studies

Elastic and viscous moduli of PLMA solutions during the photopolymerization process were studied by photorheology. Both PLMA100 and PLMA300 solutions at 10%, 15% and 20% (w/v) were used for rheological studies. A Kinexus Lab+ (Malvern Panalytical, UK) equipped with a UV curing attachment was used to characterize the photocrosslinking kinetics. The gap setting was fixed as 0.5 mm and light intensity (0.95 W/cm^2) was used for the crosslinking reaction of the precursor. Tests were performed at 25 °C with a frequency of 1.0 Hz and 0.02% of shear strain.

2.5.In vitro cell culture

2.5.1.Cell culture and encapsulation

The biological performance of PLMA hydrogels was assessed using the L929 Mouse fibroblast cell line (European Collection of Authenticated Cell Cultures (ECACC)) and human derived adipose stem cells (hASCs) (ATCC). L929 cells were cultured in Dulbecco's Modified Eagle's Medium low glucose (Sigma-Aldrich, Germany), supplemented with 10% FBS (Thermo Fisher Scientific, USA) and 1% antibiotic/antimycotic (Thermo Fisher Scientific, USA). Cells were used between passages 3 and 25. hASCs were cultured in Minimum Essential Alpha Medium (Thermo Fisher Scientific, USA) supplemented with 10% FBS (Thermo Fisher Scientific, USA) and 1% antibiotic/antimycotic (Thermo Fisher Scientific, USA). hASCs were

used until passage 5. Cell suspensions were prepared by trypsinization (trypsin/EDTA solution, Sigma-Aldrich, Germany). The cells were incorporated into the PLMA solutions to a final density of $2x10^6$ cells/mL in the case of L929 and $3x10^6$ cells/mL for hASCs. The hydrogels were prepared as described previously in section 2.3 with 6mm diameter.

2.5.2.Live/Dead assay

At pre-determined time points, hydrogels were incubated in a solution of 2µL of Calcein AM 4mM solution in DMSO (Thermo Fisher Scientific, USA) and 1µL of Propidium iodide (PI) 1 mg/mL (Thermo Fisher Scientific, USA) in 1000µL of PBS at 37ºC during 30 minutes. After washing with PBS, hydrogels were examined using a fluorescence microscope (Fluorescence Microscope Zeiss, Axio Imager 2, Zeiss, Germany).

2.5.3.Cell metabolic activity quantification

CellTiter 96® AQ_{ueous} One Solution Cell Proliferation Assay (Promega, USA) (MTS) was used to quantify the metabolic activity. After each time point, hydrogels were washed with PBS and incubated in a solution of MTS reagent diluted in PBS following manufacturer instructions. Samples were then incubated overnight at 37ºC, protected from light. The quantification was achieved by measuring absorbance at 490nm (Microplate Reader - Synergy HTX with luminescence, fluorescence and absorbance, Biotek, USA). Triplicates were made for each sample and per culturing time.

2.5.4.Cell proliferation by DNA quantification

DNA quantification was performed using a Quant-iT PicoGreen dsDNA kit (Thermo Fisher Scientific, USA). Briefly, at pre-determined time-points hydrogels were washed with PBS, incubated in sterile deionized water and frozen at -80ºC. In order to induce disruption of the cells encapsulated in the hydrogel, the samples were thawed at 37ºC and placed in an

ultrasounds bath during approximately 30 minutes. DNA standards were prepared with concentrations ranging between 0 and 2 µg/mL. The plate was incubated for 10 min in the dark and fluorescence was measured using an excitation wavelength of 480 nm and an emission wavelength of 528 nm (Microplate Reader - Synergy HTX with luminescence, fluorescence and absorbance, Biotek, USA). Triplicates were made for each sample and per culturing time.

2.5.5.Cell morphology analysis

DAPI/Phalloidin staining was made in order to access the morphology of encapsulated cells. At pre-determined time-points hydrogels were washed with PBS and fixed with a 4% formaldehyde (Sigma-Aldrich, Germany) solution during at least 2 hours. For DAPI/Phalloidin staining, a phalloidin solution (Flash Phalloidin™ Red 594, 300U, Biolegend, USA) was diluted 1:40 PBS and hydrogels were incubated at room temperature in phalloidin solution during 45 min. After washing with PBS a DAPI (4',6-diamidino-2-phenylindole dihydrochloride, Thermo Fisher Scientific, USA) solution was diluted in 1:1000 PBS and hydrogels were incubated during 5 minutes in this solution at room temperature. After washing with PBS, hydrogels were examined using a fluorescence microscope (Fluorescence Microscope Zeiss, Axio Imager 2, Zeiss, Germany).

2.5.6.Immunocytochemistry

hASCs were encapsulated in PLMA hydrogels and cultured during 7 days as described in 2.5.1. After 7 days of culture hydrogels were washed with PBS and fixed with a 4% formaldehyde (Sigma-Aldrich, Germany) solution during at least 2 hours. Following fixation, hydrogels were washed with PBS and permeabilized with 0.5% Triton X-100 BioXtra (Sigma-Aldrich, Germany) in PBS during 30 minutes. Then hydrogels were washed with PBS and blocked with 0.5% FBS (Thermo Fisher Scientific, USA) in PBS during 1 hour. Alexa Fluor® 647 anti-human CD90 (Thy1) Antibody (BioLegend, San Diego, CA) and PE anti-human CD73

(Ecto-5'-nucleotidase) Antibody (BioLegend, San Diego, CA) were diluted in 0.5% FBS in PBS and incubated overnight at 4ºC. After washing with PBS a DAPI (4',6-diamidino-2-phenylindole dihydrochloride, Thermo Fisher Scientific, USA) solution was diluted in 1:1000 PBS and hydrogels were incubated during 5 minutes in this solution at room temperature to fluorescently label the nuclei. After washing with PBS, hydrogels were examined using a fluorescence microscope (Fluorescence Microscope Zeiss, Axio Imager 2, Zeiss, Germany).

2.6.Quantification of protein and GFs release from PLMA hydrogels

For the protein release assays, six samples of each PLMA100 at 10% and 15% (w/v) were made. Samples were added to falcons with 5 mL of PBS (Thermo Fischer Scientific, USA). The samples were incubated in a bath at 37ºC with constant agitation (60 rpm). At each time point, an aliquot of 600 µL was taken from each sample and 600 µL of fresh PBS added. Collected samples were stored at -20ºC. Total protein quantification was performed with Micro BCA Protein Assay Kit (Thermo Fisher Scientific, USA). ELISA quantification of fibrinogen (Human Fibrinogen ELISA Kit, abcam, UK) and VEGF (VEGF Human ELISA Kit, Invitrogen™, ThermoFisher Scientific, USA) was also performed.

2.7.Fabrication of PLMA microstructures

Lyophilized PLMA100 was dissolved with 0.5% (w/v) 2-hydroxy-4'-(2-hydroxyethoxy)-2-methylpropiophenone (Sigma-Aldrich, Germany) in PBS (Sigma-Aldrich, Germany) to a final concentration of 15% (w/v). 50µL of this solution were poured onto a glass coverslip. Then, a photomask was brought into contact with the solution and gently pressed. The photomask was exposed to UV irradiation (0.95 kW/cm^2) during 60s. The photomask was then removed from the glass. PLMA microstructures were labeled by incubation in 1mL of Fluorescein 5(6)-isothiocyanate (FITC) (1 µg/mL) (Sigma-Aldrich, Germany) in PBS (Sigma-Aldrich, Germany) and Rhodamine B isothiocyanate (1 µg/mL) (Sigma-Aldrich, Germany) in

PBS (Sigma-Aldrich, Germany). After 10 minutes of incubation the microstructures were washed with PBS (Sigma-Aldrich, Germany) and visualized using a fluorescence microscope (Fluorescence Microscope Zeiss, Axio Imager 2, Zeiss).

2.8.Statistical analysis

All data were subjected to statistical analysis and were reported as a mean ± standard deviation. Statistical differences between the analyzed groups were determine by two-tailed unpaired *t* test where $P < 0.01$ were considered as significant. All statistical analysis was performed using GraphPad Prism software.

3.Results and discussion

3.1.Synthesis and PLMA characterization

Human platelets are an important autologous source of multiple proteins, GFs and cytokines that can be extracted by platelet lysis.[27] In this study, photopolymerizable Platelet lysates (PL) based hydrogels with tunable physical properties that can be used for cell encapsulation or as substrates for two-dimensional (2D) cell culture were synthesized for the first time. Methacryloyl platelet lysates (PLMA) were synthesized by reaction of PL with MA. Based on previously published works on the modification of gelatin and tropoelastin with methacrylate groups[7,28–32], we developed a protocol for the synthesis of PL proteins modified with methacryloyl groups. Proteins present in PL have amino and hydroxyl groups susceptible to react with methacrylic anhydride – see figure 1A. Different degrees of methacrylation could be obtained by varying the molar ratio of MA to PL concentration. In this work two degrees of modification were synthesized: low degree of modification (PLMA100) and high degree of modification (PLMA300). The degree of conversion with MA groups (i.e. degree of methacrylation) in biopolymers has conventionally been determined using ^{1}H NMR spectroscopy. Despite the complex variety of proteins and GFs in PL, ^{1}H NMR analysis to

PLMA confirmed the methacrylation of PL by the appearance of distinctive peaks in the double bound region (δ 5.2 – 5.6 ppm) (figure 1B) and a sharp peak that corresponds to the -CH_3 of the methacrylate groups (δ ≈ 2 ppm) (figure 1B) on the modified PL spectra.

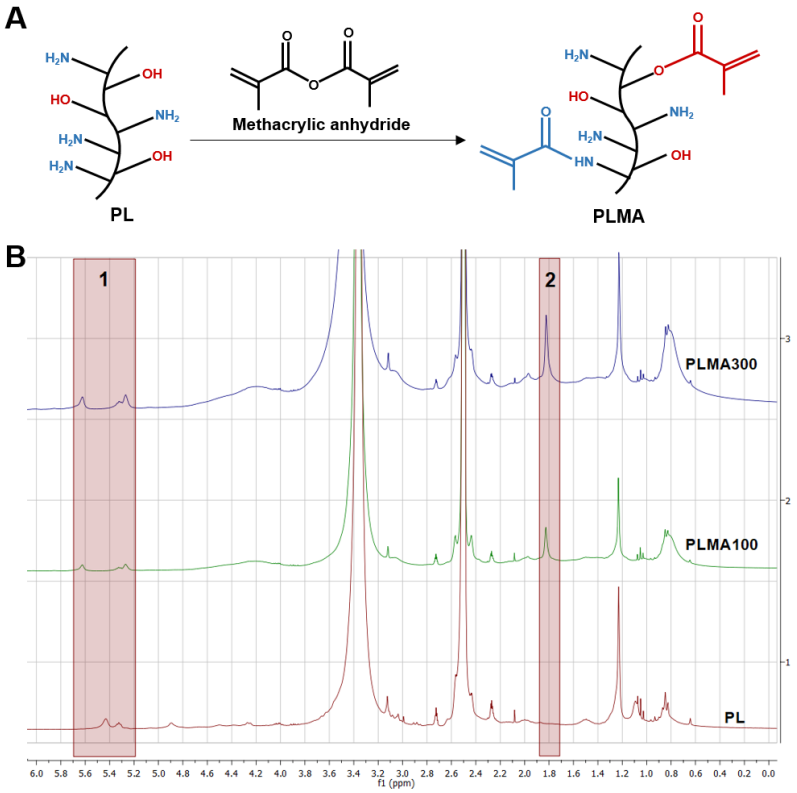

Figure 1. A) Methacrylate and methacrylamide groups inserted after reaction of PL with methacrylic anhydride. B) ^{1}H NMR spectra of PL, PLMA100 and PLMA300 with distinctive peaks characteristics of methacrylate groups: double bound methacrylate (1) and -CH_3 of methacrylate group (2).

For a more accurate analysis of the protein modifications, mass spectrometry was also performed. Platelets contain more than 1100 different proteins, with numerous post-translational modifications, resulting in over 1500 protein-based bioactive factors.[33] Table 1 summarizes the main components found in the original PL and PLMA samples starting from the most abundant protein (N=1). Results demonstrated that the main components of PL did not significantly change upon conjugation of proteins with methacryloyl groups. Results also show that human serum albumin is the most abundant protein in both PL and PLMA.

PL	PLMA100	PLMA300

N	Protein	Protein	Protein
1	Serum albumin	Serum albumin	Serum albumin
2	Apolipoprotein B-100	Serotransferrin	Complement C3
3	Complement C3	Complement C3	Serotransferrin
4	α2 macroglobulin	α2 macroglobulin	α2 macroglobulin
5	Serotransferrin	Keratin type II cytoskeletal 1	Apolipoprotein B-100
6	Complement C4-B	Apolipoprotein B-100	Keratin, type II cytoskeletal 1
7	Keratin type I cytoskeletal 10	Keratin type I cytoskeletal 9	α1 antitrypsin
8	Immunoglobulin γ1 heavy chain	Apolipoprotein A-I	Keratin type I cytoskeletal 10
9	Keratin type II cytoskeletal 1	Keratin type I cytoskeletal 10	Haptoglobin
10	Apolipoprotein A-I	Haptoglobin	Apolipoprotein A-I
11	α1 antitrypsin	Immunoglobulin γ1 heavy chain	Complement C4-B
12	Haptoglobin	α1 antitrypsin	Immunoglobulin γ1 heavy chain
13	Keratin type II cytoskeletal 2 epidermal	Keratin type II cytoskeletal 2 epidermal	Keratin type II cytoskeletal 2 epidermal
14	Ceruloplasmin	Immunoglobulin heavy constant mu	Ceruloplasmin
15	Keratin type I cytoskeletal 9	Immunoglobulin heavy constant α1	Keratin type I cytoskeletal 9
16	Apolipoprotein A-IV	Ceruloplasmin	Immunoglobulin heavy constant um
17	Hemopexin	Hemopexin	Hemopexin
18	Immunoglobulin mu heavy chain	Inter α-trypsin inhibitor heavy chain H4	α1-B-glycoprotein
19	Complement factor B	Keratin type II cytoskeletal 5	Immunoglobulin heavy constant α1
20	Complement factor H	Antithrombin-III	Inter α-trypsin inhibitor heavy chain H4
21	Immunoglobulin heavy constant alpha 1	Keratin, type I cytoskeletal 14	Actin, cytoplasmic 2
22	Vitamin D-binding protein	α1-B-glycoprotein	Immunoglobulin kappa light chain
23	Complement C5	Actin cytoplasmic 2	Transthyretin
24	Actin cytoplasmic 2	Immunoglobulin kappa light chain	Apolipoprotein A-IV
25	α1-B-glycoprotein	Immunoglobulin heavy constant γ2	Inter-α-trypsin inhibitor heavy chain H2
26	Fibrinogen γ chain	Complement factor B	Antithrombin-III
27	Fibrinogen α chain	α1-acid glycoprotein 1	Vitamin D-binding protein
28	Inter-α-trypsin inhibitor heavy chain H4	Vitronectin	α1-antichymotrypsin
29	Inter-α-trypsin inhibitor heavy chain H2	Inter-α-trypsin inhibitor heavy chain H1	Complement factor B
30	Immunoglobulin kappa light chain	Kininogen-1	Plasma protease C1 inhibitor
31	α1-antichymotrypsin	Fibrinogen γ chain	Apolipoprotein E
32	Antithrombin-III	α1-antichymotrypsin	Immunoglobulin heavy constant γ2
33	Prothrombin	Complement C4-B	Vitronectin
34	Apolipoprotein E	Apolipoprotein A-IV	Fibrinogen γ chain
35	Fibrinogen β chain	Angiotensinogen	Angiotensinogen

Table 1. Main components found in PL, PLMA100 and PLMA300 by mass spectrometry analysis, listed according to their relative abundance.

Based on the mass spectrometry results showing the main proteins found in PL, it was calculated the relative peptide content (%) compared with the total peptides found in PL. Figure 2 represents the relative percent of peptides found for each protein compared with the total amount of peptides.

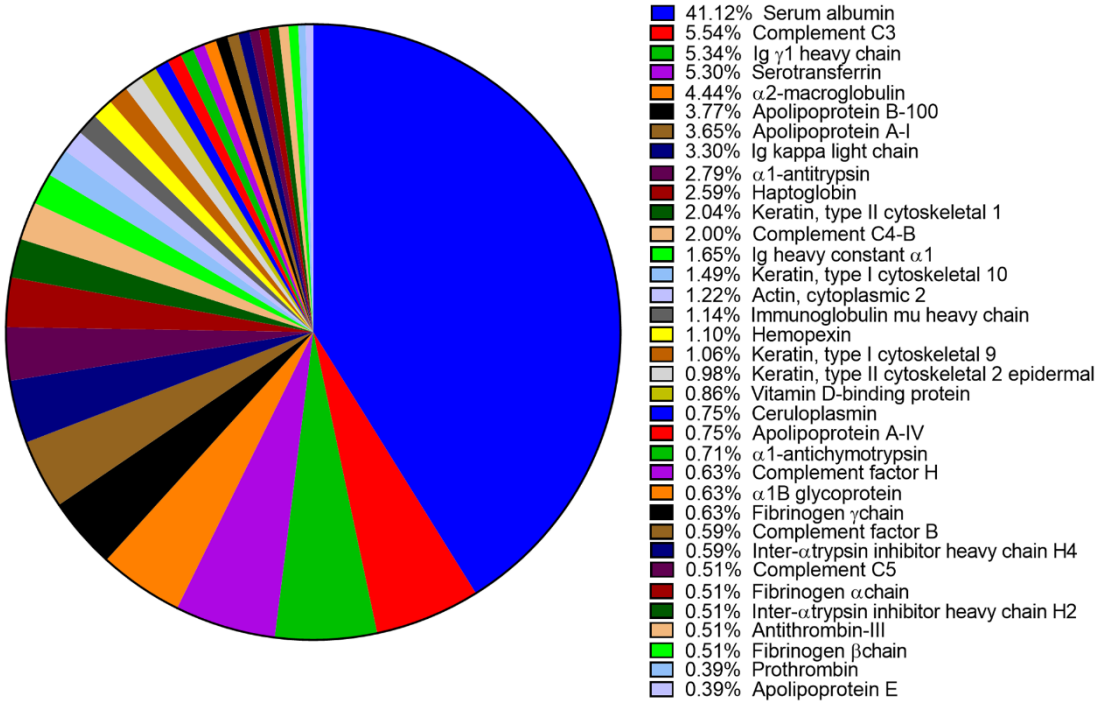

Figure 2. Relative percent of peptides found in original PL for each main protein compared with the total amount of found peptides.

The total peptide sequences per formulation (PLMA100 and PLMA300) and the amount of modified peptide sequences was obtained by mass spectrometry. The degree of modification was then estimated by dividing the amount of modified peptide sequences by the total peptide sequences. As it was expected, mass spectrometry results for PLMA100 reveals less modified peptides with methacryloyl groups than in PLMA300 (table 2) and most of these modification sites occur in serum albumin peptides (figure 3). Mass spectroscopy results reveal that modification occurs in different residues but mainly in lysine (K) and glutamine (Q) residues, as it was previously reported for the modification of gelatin and tropoelastin with this type of chemical conjugation.[31]

Sample	Total peptide sequences	Modified peptide sequences	Degree of modification
PLMA100	2410	346	14%
PLMA300	3391	846	25%

Table 2. Mass spectrometry results for total number of identified peptides and also the number of modified peptides found.

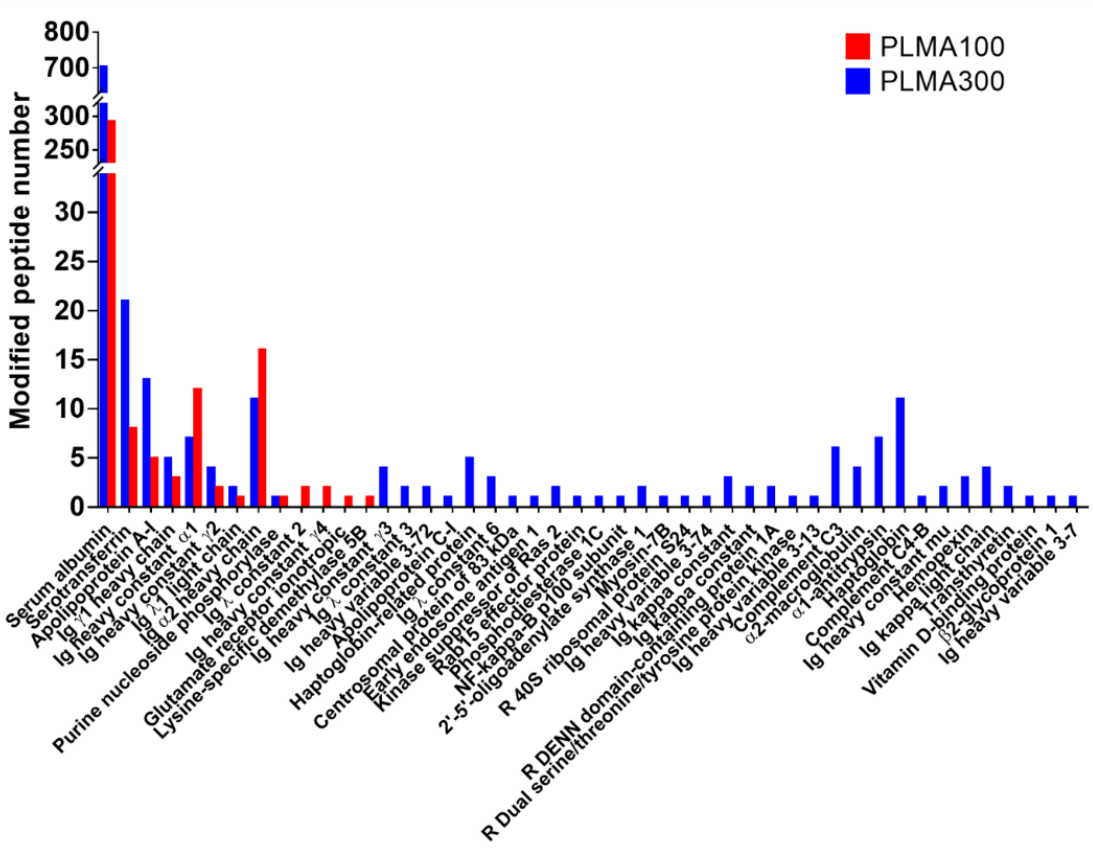

Figure 3. Modified peptides for each protein found in PLMA100 and PLMA300.

3.2.Hydrogel formation

Hydrogels were easily and rapidly formed by photopolymerization upon exposure of PLMA solution to UV irradiation. The obtained PLMA formulation is water soluble and its low viscosity allow the preparation of PLMA solutions up to 20% (w/v). This characteristic is especially important in injectable hydrogels as this way its application is easier and requires minimally invasive procedures. Another important characteristic of these hydrogels is the fact that the total crosslinking occurs in 30s to 60s of UV exposure at quite low intensity, 0.95 W/cm^2. Figure 4 shows PLMA hydrogels for each modification degree at 10%, 15% and 20% (w/v).

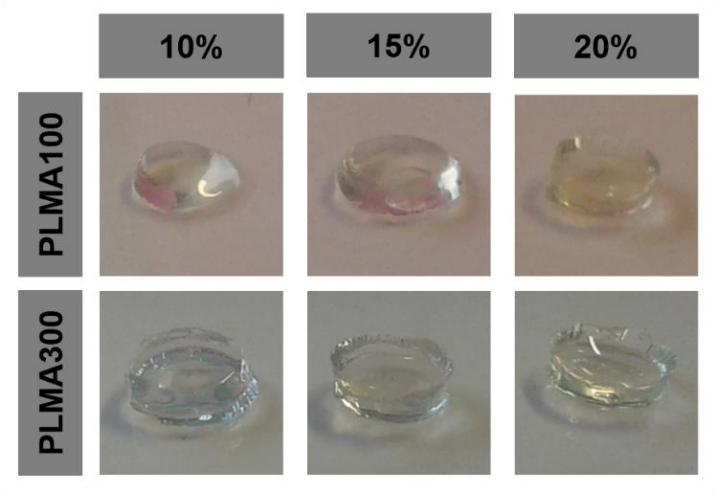

Figure 4. Photocrosslinked PLMA hydrogels formed from PLMA100 and PLMA300 at 10%, 15% and 20% (w/v).

3.3.Characterization of PLMA hydrogels

3.3.1.Structural properties of PLMA hydrogels

Hydrogels porosity influences nutrient flux throughout the matrix and is related with hydrogel swelling and mechanical properties.[34] Small molecular porosity is correlated with lower swelling ratio and higher modulus.[34–36] Molecular porosity and mechanical properties of hydrogels are important characteristics that have to be taken into account due to its influence in cell behavior. Penetration of cells into hydrogels, as well as migration, proliferation and exchange of oxygen, nutrients and waste materials are processes influenced by hydrogel stiffness.[37,38] In order to explore PLMA hydrogels microstructure, SEM analysis of lyophilized PLMA gels was performed. These structures have a porous network influenced by PLMA concentration and also modification degree, as showed in figure 5A-B. Results also show that PLMA hydrogels have a heterogenic structure with respect to porosity with a slight decrease in pore size with the increase in PLMA concentration for PLMA100. The diminution in pore size with the increase of PLMA concentration is more significant for PLMA300, from an average pore size at PLMA300 10% (w/v) of ~10 µm up to ~5 µm at PLMA300 20% (w/v).

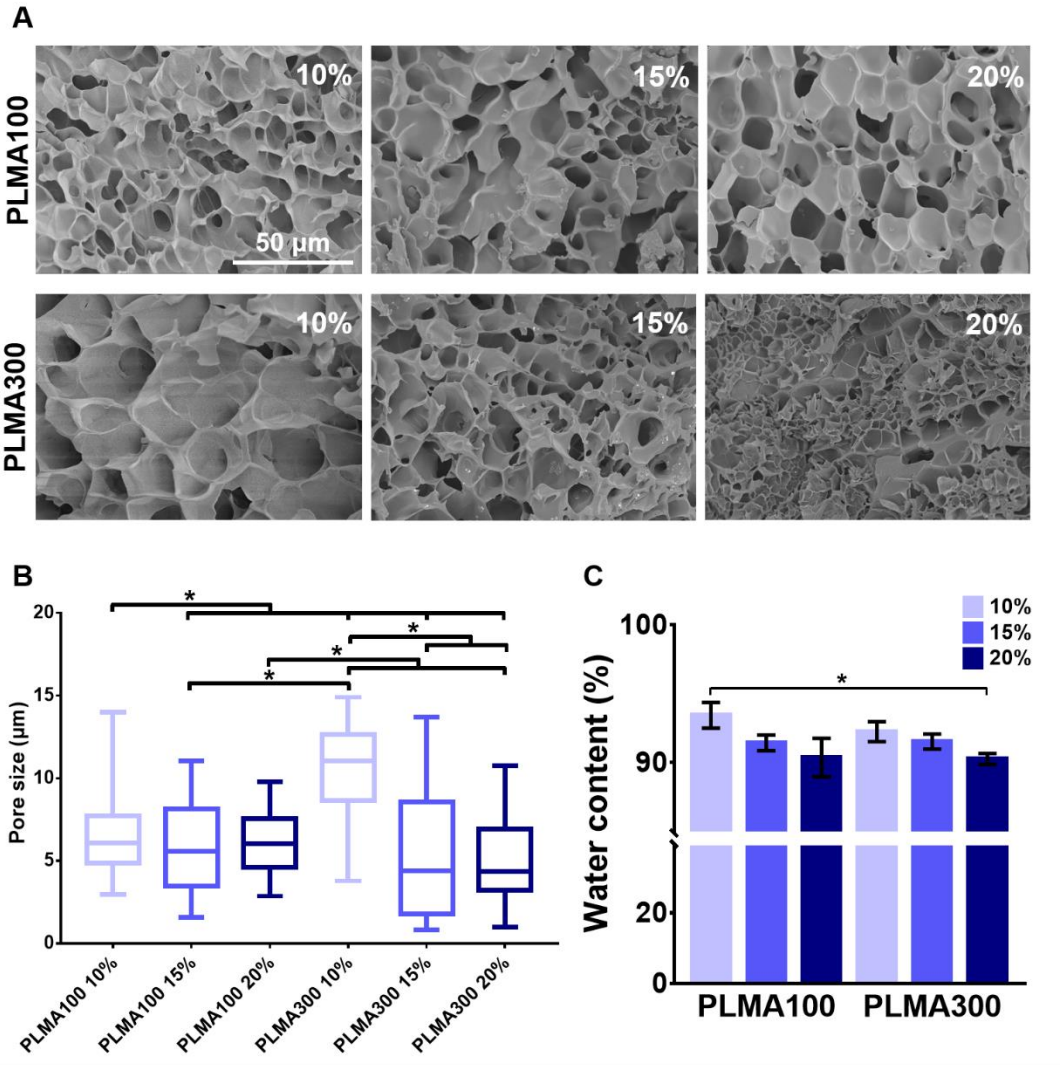

Figure 5. (A) Representative cross-section SEM images of PLMA100 and PLMA300 hydrogels. (B) Pore size values obtained for PLMA100 and PLMA300. (C) Water content for PLMA100 and PLMA300 hydrogels. All studies were performed for PLMA100 and PLMA300 hydrogels at 10%, 15% and 20% (w/v). Statistical analysis through two-tailed unpaired *t* test showed significant differences (*P < 0.01) between the analyzed groups.

The porosity of PLMA hydrogels is not very different from other protein based hydrogels like gelatin methacryloyl and it can be tuned by changing some hydrogel fabrication parameters[37], which does not occur for other hydrogels like tropoelastin methacrylate based hydrogels where pore size is not very different for each low modification degree concentration.[32]

The water content of PLMA hydrogels was also evaluated. Results shown that this parameter is not significantly influenced by the degree of modification or PLMA concentration. In general, PLMA hydrogels have more than 90% of water content (Figure 5C).

3.3.2.Mechanical and rheological characterization

PL based gels formed upon activation of PL concentrates with calcium and thrombin have been used as materials for cell culture.[39,40] Nevertheless, these hydrogels typically present poor mechanical properties and are difficult to handle. Moreover, they tend to degrade fast *in vitro*, unless some antifibrinolytic agent is used in order to slow down the degradation process.[41] On the other side, animal based materials such as collagen and the mixture of proteins derived from the EHS tumor, widely used as cell culture matrices have issues with handling and own potential immunogenicity. To overcome these limitations, the human based hydrogels here proposed may be easily tuned to present enhanced stability and well controlled mechanical properties.

Rheological measurements were performed for PLMA100 and PLMA300 at 10%, 15% and 20% (w/v) to study the photopolymerization process of PLMA materials – see figure 6. The storage modulus increases with the increase in concentration or degree of modification – see figure 6A and 6B. Figure 6C presented the time needed to achieve an hydrogel with a modulus approximately half of the final ($t_{1/2}$). For each condition, $t_{1/2}$ decreases with an increase in PLMA concentration or degree of modification, possibly due to the higher availability of double bounds to induce crosslinking. tan δ gives the ratio between the storage modulus (G') and the loss modulus (G''). These values, between 0.05 and 0.2, clearly demonstrate the viscoelastic nature of the resulting hydrogels. tan δ increases with increasing concentration and degree of modification, therefore increasing the damping capability of the hydrogel.

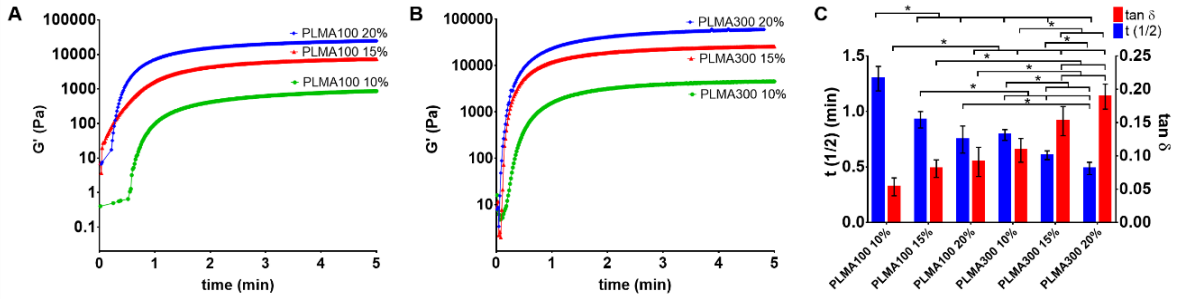

Figure 6. Representative curves for storage modulus (G') for PLMA100 (A) and PLMA300 (B). (C) $t_{1/2}$ and tan δ for PLMA100 and PLMA300. All studies were performed for PLMA100 and PLMA300 hydrogels at 10%, 15% and 20% (w/v). Statistical analysis through two-tailed unpaired *t* test showed significant differences (*P < 0.01) between the analyzed groups.

We also tested PLMA hydrogels mechanical properties and how they change by varying PLMA modification degree and concentration. As for rheological measurements, compressive mechanical tests were performed in hydrogels made from PLMA100 and PLMA300 at 10%, 15% and 20% (w/v). Figure 7A shows the compressive stress-strain results of PLMA hydrogels. The data shown in figure 7B shows how Young's modulus increases with the increase in the PLMA concentration. Likewise, an increase in the degree of modification of PL, corresponds to an increase in stiffness for the same concentration of polymer. Young's modulus of PLMA100 is lower for all concentration tested when compared with the same concentrations of PLMA300 hydrogels. Figure 7C shows the ultimate strain (%) for PLMA hydrogels and the influence of polymer concentration and degree of modification on these values. The ultimate strain is higher in PLMA at lower concentration (10% (w/v)). Comparing data obtained for both degrees of modification the ultimate strain is higher in PLMA100 hydrogels than in PLMA300. PLMA300 hydrogels have less resistance to fracture compared to PLMA100. This may be due to the higher degree of methacrylation, which increases the crosslinking density of hydrogels and also its stiffness.[35] Figure 7D shows the ultimate stress for each concentration of two different modification degrees. An increase in the ultimate stress from the 10% (w/v) to 20% (w/v) hydrogels is evident. It is important to point out that PLMA hydrogels are formed rapidly

within 30 - 60 seconds upon UV irradiation, which is shorter than the typical time (~ 20min - 1h) required to crosslink PRP-based gels with calcium and thrombin.[42]

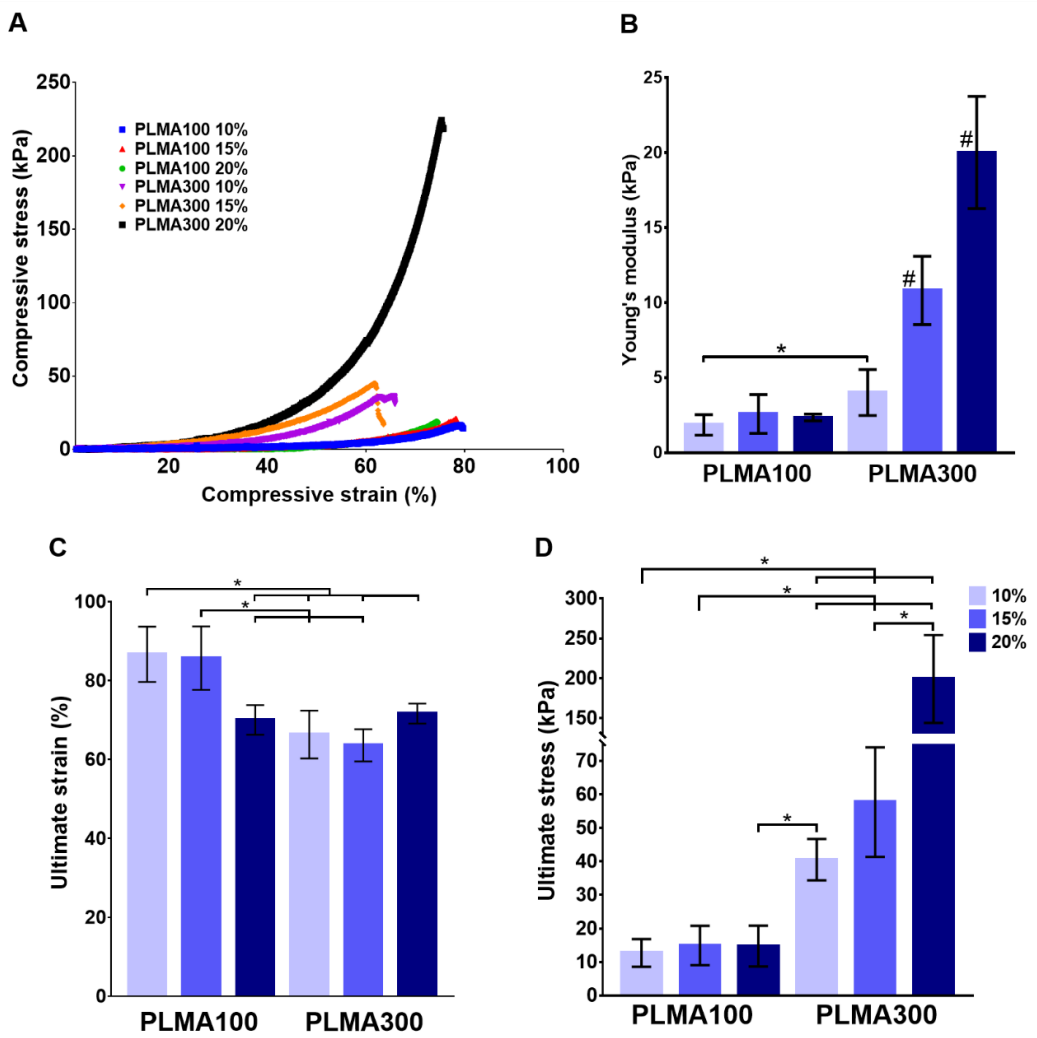

Figure 7. (A) Representative compressive stress-strain curves for PLMA100 and PLMA300 hydrogels. (B) Young's modulus, (C) ultimate strain and (D) ultimate stress results for PLMA100 and PLMA300. All studies were performed for PLMA100 and PLMA300 hydrogels at 10%, 15% and 20% (w/v). Statistical analysis through two-tailed unpaired *t* test showed significant differences (*P < 0.01) between the analyzed groups (#, significantly different from all the others on the left).

3D cell culture platforms such as hydrogels have to provide ideal features to support cell adhesion and proliferation, this way mimicking the *in vivo* extracellular

microenvironment.[34,43,44] In particular, the mechanical properties play a key role in the *in vitro* integrity of the hydrogel and in cellular mechanotransduction, this way affecting cellular spreading, migration and also differentiation.[45] PLMA hydrogels have unique structural properties that allow them to behave as a viscoelastic solid with improved mechanical properties compared to PRP based gels so far reported.[42] The Young's modulus of the herein reported hydrogels may be tuned in the range of 0.5 – 20 kPa. Therefore, the developed PLMA hydrogels can be used to mimic some native tissues with known stiffness between these Young's modulus values such as: brain tissue (elasticity 0.1-1 kPa)[43,46] and striated muscle (elasticity 8-17 kPa).[47]

3.4.In vitro cell culture studies

L929 mouse fibroblasts were used for a first screening of the biological performance of the PLMA hydrogels. Cells encapsulated in PLMA100 hydrogels at 10% (w/v) were cultured during 7 days and at determined time points, namely 1, 3 and 7 days, analysis to cell morphology, viability and proliferation was performed. Figure 8A shows that cells are well distributed within the hydrogel, exhibiting high viability and elongated morphology at day 1 and day 7. DAPI/Phalloidin staining was also performed at days 3 and 7 in order to evaluate cell morphology inside the PLMA hydrogels (figure 8B-C). It is perfectly clear that L929 cells adhered, spread and proliferated within the PLMA hydrogel.

In a second assay, hASCs were used in order to test the potential of PLMA hydrogels to support the culture of human derived stem cells. In a first approach, hydrogels made of PLMA100 at 10% (w/v) hydrogels were used for hASCs encapsulation likewise for L929 culture. However, the results revealed that these hydrogels do not properly promote hASCs adhesion and proliferation. Based on literature reports that suggest stiffer hydrogels for increased hASCs adhesion and proliferation[48,49], PLMA100 hydrogels at a 15% (w/v) concentration were tested. Live/Dead assay reveal that PLMA hydrogels greatly support cell

viability up to 7 days in culture (figure 8A). Cell morphology was assessed by DAPI/Phalloidin staining at 3 and 7 days of culture (Figure 8B-C). After 3 days in culture, cells readily elongated in PLMA hydrogels and after 7 days in culture cells are perfectly elongated and migrated, forming interconnected networks with neighboring cells. Immunocytochemistry analysis of hASCs at 7 days of cell culture with stem cell specific biomarkers (CD90 and CD73) show no evidence of differentiation of hASCs encapsulated in PLMA hydrogels.

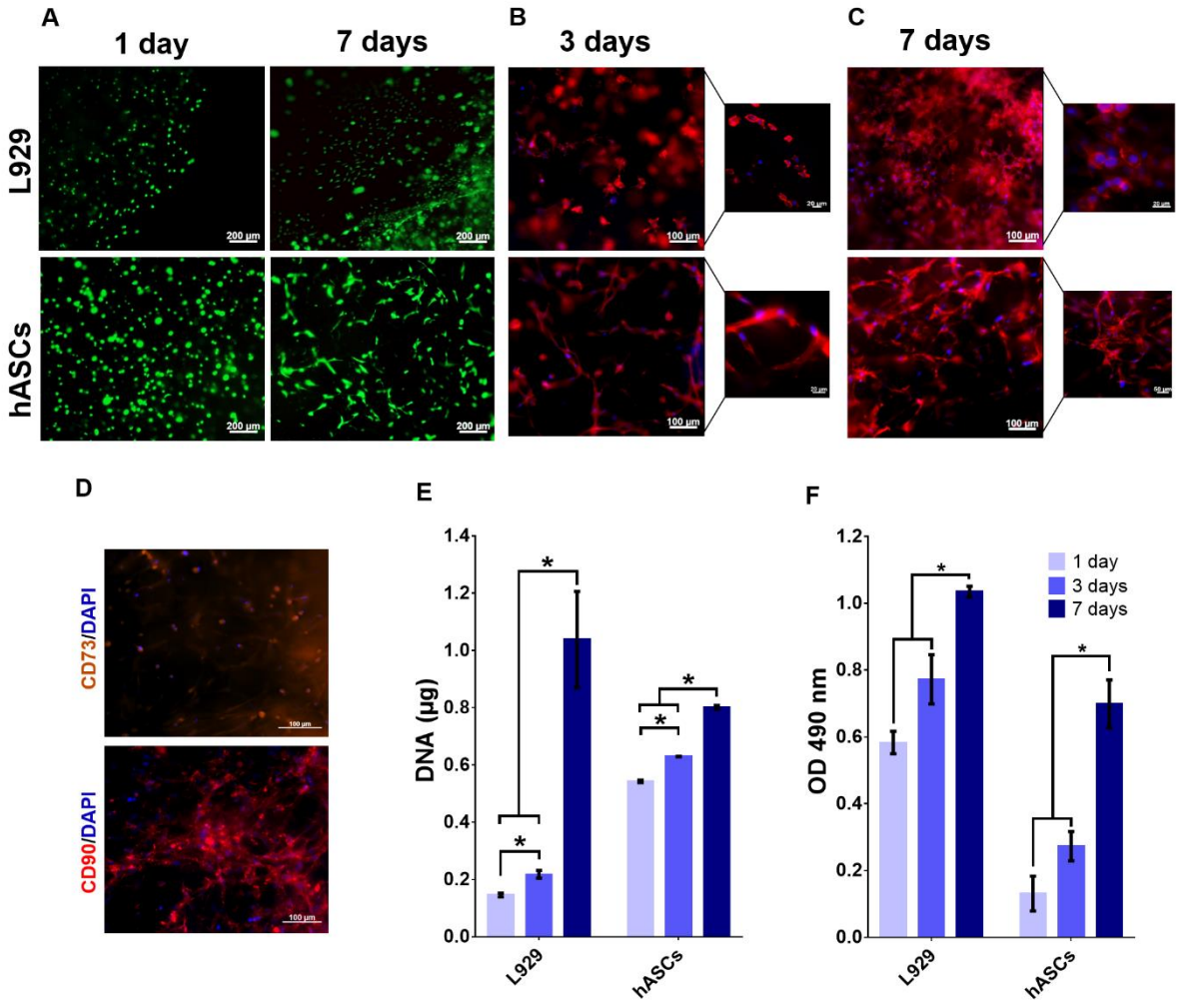

Figure 8. Representative fluorescence images for: (A) L929 encapsulated in PLMA100 10% (w/v) and hASCs encapsulated in PLMA100 15% (w/v) live/dead at 1 and 7 days of culture in. (B) and (C) L929 and hASCs DAPI/Phalloidin staining at 3 and 7 days of cell culture. (D) Immunocytochemistry images of hASCs with CD90/DAPI and CD73/DAPI at 7 days of cell culture. DNA (E) and MTS (F) results for L929 and hASCs at 1 day, 3 and 7 days of cell culture. Statistical analysis through two-tailed unpaired *t* test showed significant differences (*P < 0.01) between the analyzed groups.

Cell proliferation and cell viability assays were performed by DNA quantification (Figure 8D) and MTS assay (Figure 8E), respectively. L929 as well as hASCs are able to proliferate inside PLMA hydrogels as it can be seen by the increasing in DNA content and also by the results for metabolic activity analysis. These results are in agreement with previously described results for live/dead assay and DAPI/Phalloidin staining (figure 8A, 8B and 8C), which demonstrated cell spreading and proliferation within PLMA hydrogels. Cells maintain their viability for at least 7 days and are able to proliferate inside the hydrogels.

Depending on the cell type, a specific stiffness of PLMA hydrogels may be required, this is easily adjusted by varying degree of modification or PLMA precursor concentration. For example, hASCs adhesion was poor on 10% (w/v) PLMA100 hydrogels, when the same cells were encapsulated within PLMA100 15%, they rapidly adhere and spread within the hydrogels.

Cell migration through ECM is critical in a variety of physiologic and pathophysiologic situations. Here we propose proteolytically degradable human ECM derived hydrogels as a 3D cell culture platform. Such biodegradable and bioresponsive hydrogels are therefore promising materials that can be used for 3D cell culture, in particular to engineer human microtissues or for the development of humanized *in vitro* disease models.

3.5.Microfabrication of PLMA based hydrogels

Photopolymerizable hydrogels permit to fix the shape of the solution precursor using light. Microfabricated structures of PLMA hydrogels were obtain by photopolymerization of PLMA100 15% (w/v) solution using a photomask (figure 9A). PLMA was processed to create microstructures with multiple geometries that may be further assembled (figure 9B). These results support the idea that PLMA hydrogels can be manipulated according to user-defined 3D microstructures in cell-laden microgels and eventually assembled into larger structures to mimic the tissue hierarchical organization, using bottom-up tissue engineering strategies.[50]

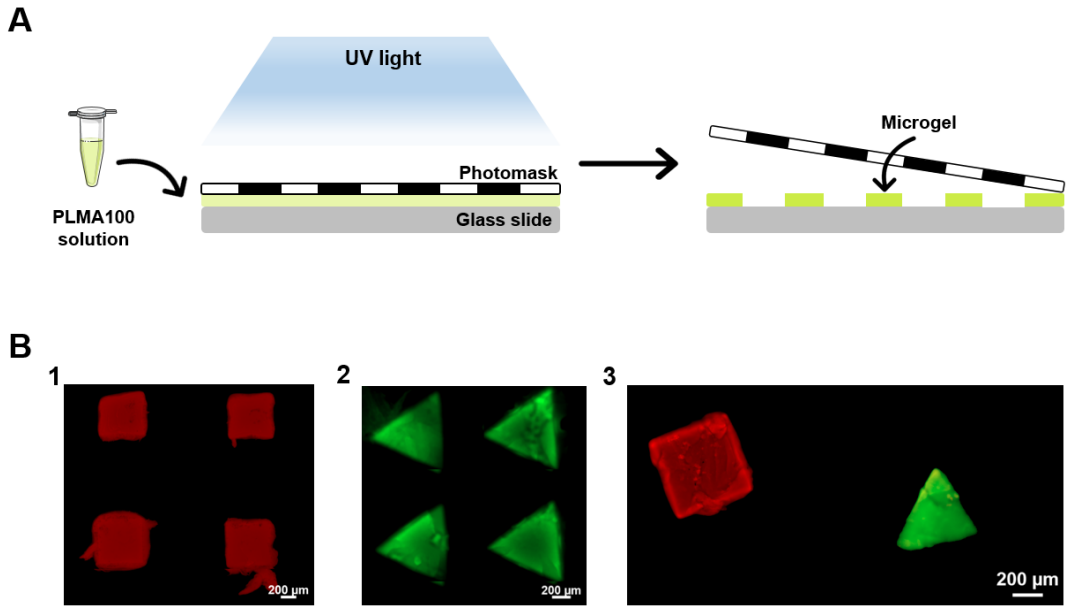

Figure 9. (A) Procedure to generate microgels with higher tuned geometry and size. (B) Representative fluorescence images for: (1) PLMA microgels labeled with FITC; (2) PLMA microgels labeled with rhodamine B isothiocyanate; (3) PLMA microgels in suspension after detachment from the glass slide.

3.6.Release of bioactive molecules from PLMA hydrogels

PLMA hydrogels here described are a pool of proteins, GFs and other molecules that are essential for cell adhesion, growth and proliferation. We predicted that a fraction of this complex mixture of proteins will be loosely bounded to the hydrogel after the photocrosslinking step. For this reason, protein and GFs release assays were performed in order to identify the release profile from PLMA hydrogels. Figure 10A shows the total protein release profile from the gels used for *in vitro* cell encapsulation assays, PLMA100 at 10% and 15% (w/v). Protein release profile of PLMA hydrogels shows an overall sustained release. In the first 24 hours of the assay, protein release is quite fast, then between 24h and approximately 240h protein release is well sustained. It is also important to refer that the hydrogels maintain their shape during the time release tests were performed. Using an autologous or allogeneic source of GFs instead of recombinant GFs, which are very expensive and have a short half-life, has already been proposed.[51–53] PLMA hydrogels are a pool of human GFs and they can be potentially used as a platform for the release of autologous or allogeneic GFs and bioactive proteins involved in

cell recruitment, growth and proliferation processes. The vascular endothelial growth factor (VEGF) is an inducer of angiogenesis that has been long recognized as an important and necessary step during tissue repair.

On the other hand, fibrinogen has been recognized as a main component in PRP and is a key element in the previous reported PRP based gels. Thus, ELISA assay was performed to investigate the release profile of both VEGF and fibrinogen from the PLMA hydrogels. As well as in total quantification, the release of fibrinogen and VEGF occurs in a sustained manner, as shown in figure 10B. Typically VEGF concentrations of 5, 10 or 20 ng/mL induced a 2-2.5-fold increase in proliferation and migration of endothelial cells in comparison with no VEGF. The amount of VEGF released from the hydrogels is quite below these values, further studies will be performed to evaluate the bioactivity of immobilized VEGF within the hydrogel and its influence in endothelial cell proliferation and migration. The low amount of fibrinogen released from the hydrogel, suggest that this protein is a key structural component of the PLMA structures and covalently bonded to the hydrogel network.

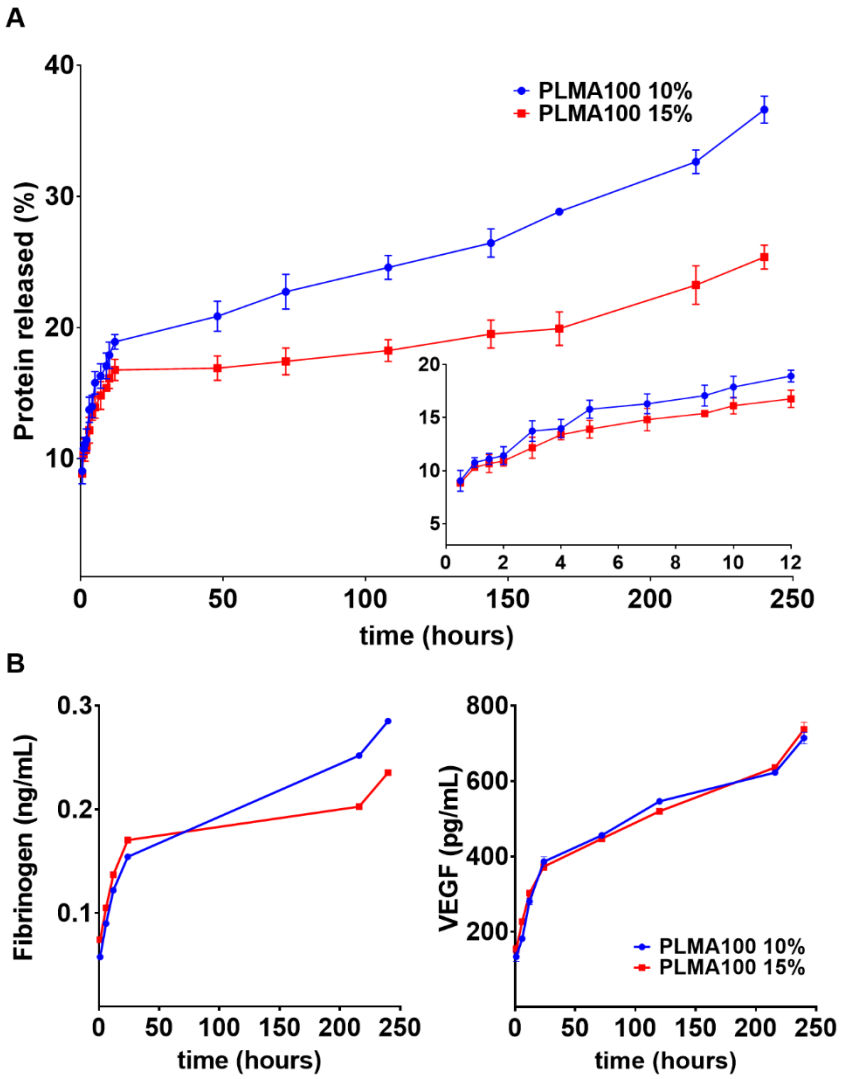

Figure 10. Total protein release quantification (A) and ELISA quantification of fibrinogen and VEGF (B) for PLMA100 10% and 15% (w/v).

4.Conclusion

PRP and PL are attractive sources of GFs that have been widely studied for TE applications. Previous studies found in the literature concerning the use of hydrogels based on PRP, mostly report the activation with thrombin and crosslinking with calcium. Despite the potential of those systems, the limited mechanical properties, and low stability *in vitro* results in an ineffective strategy. Herein we reported, for the first time, a direct modification of PL proteins with a photoresponsive group. Such modification allow the production of PL derived photopolymerized hydrogels with tunable mechanical and biochemical properties. The PLMA

based hydrogels here proposed not only have increased mechanical properties but also higher stability *in vitro* when compared to PRP/PL based reported materials. PLMA based hydrogels support the adhesion and proliferation of encapsulated cells. Our results suggest that such type of gels may be an alternative to collagen and proteins derived from the Engelbreth-Holm- EHS tumor, the gold standards to provide 3D cell cultures for a wide range of cell types. A foremost advantage of PLMA based gels is their human origin, following the current animal-free approaches and autologous or allogenic strategies for cell culture and biomedical applications. Recognizing the unprecedented potential of the PLMA gels to support 3D cell culture, we hypothesize that PLMA based gels may be used as cell culture platforms avoiding the use of animal derived supplements.

Acknowledgements

This work was supported by European Research Council grant agreement ERC-2017-PoC-789760 for project MicroBone.
The authors acknowledge the UniMS – Mass Spectrometry Unit, ITQB/iBET, Oeiras, Portugal, for providing data and analysis for Mass Spectrometry.

Received: ((will be filled in by the editorial staff))
Revised: ((will be filled in by the editorial staff))
Published online: ((will be filled in by the editorial staff))

References

[1] K. Duval, H. Grover, L.-H. Han, Y. Mou, A. F. Pegoraro, J. Fredberg, Z. Chen, *Physiology* **2017**, *32*, 266.

[2] R. Edmondson, J. J. Broglie, A. F. Adcock, L. Yang, *Assay Drug Dev. Technol.* **2014**, *12*, 207.

[3] H. Geckil, F. Xu, X. Zhang, S. Moon, U. Demirci, *Nanomedicine* **2010**, *5*, 469.

[4] D. Lv, Z. Hu, L. Lu, H. Lu, X. Xu, *Oncol. Lett.* **2017**, *14*, 6999.

[5] M. W. Tibbitt, K. S. Anseth, *Biotechnol. Bioeng.* **2009**, *103*, 655.

[6] K. Y. Lee, D. J. Mooney, *Chem. Rev.* **2001**, *101*, 1869.

[7] D. Loessner, C. Meinert, E. Kaemmerer, L. C. Martine, K. Yue, P. A. Levett, T. J. Klein, F. P. W. Melchels, A. Khademhosseini, D. W. Hutmacher, *Nat. Protoc.* **2016**, *11*, 727.

[8] E. H. Nguyen, W. T. Daly, N. N. T. Le, M. Farnoodian, D. G. Belair, M. P. Schwartz, C. S. Lebakken, G. E. Ananiev, M. A. Saghiri, T. B. Knudsen, et al., *Nat. Biomed. Eng.* **2017**, *1*, 1.

[9] M. G. McCoy, B. R. Seo, S. Choi, C. Fischbach, *Acta Biomater.* **2016**, *44*, 200.

[10] J. Zhu, R. E. Marchant, *Expert Rev. Med. Devices* **2011**, *8*, 607.

[11] H.-L. Wang, G. Avila, *Eur. J. Dent.* **2007**, *1*, 192.

[12] A. Altaie, H. Owston, E. Jones, *World J. Stem Cells* **2016**, *8*, 47.

[13] J. Araki, M. Jona, H. Eto, N. Aoi, H. Kato, H. Suga, K. Doi, Y. Yatomi, K. Yoshimura, *Tissue Eng., Part C* **2012**, *18*, 176.

[14] L. Frese, T. Sasse, B. Sanders, F. P. T. Baaijens, G. M. Beer, S. P. Hoerstrup, *J. Tissue Eng. Regener. Med.* **2016**, *11*, 2193.

[15] M. P. Mojica-henshaw, P. A. M. Jacobson, J. Morris, L. Kelley, J. A. N. Pierce, M. Boyer, J. Reems, *Cytotherapy* **2013**, *15*, 1458.

[16] P. Babo, V. E. Santo, A. R. C. Duarte, C. Correia, M. H. G. Costa, J. F. Mano, R. L. Reis, M. E. Gomes, *Inflammation Regener.* **2014**, *34*, 33.

[17] X. Xie, Y. Wang, C. Zhao, S. Guo, S. Liu, W. Jia, R. S. Tuan, C. Zhang, *Biomaterials* **2012**, *33*, 7008.

[18] S. C. Santos, O. E. Sigurjonsson, C. A. Custódio, J. F. Mano, *Tissue Eng., Part B* **2018**, 1.

[19] P. Gentile, M. G. Scioli, A. Bielli, A. Orlandi, V. Cervelli, *Stem Cells* **2017**, *35*, 117.

[20] R. El Backly, V. Ulivi, L. Tonachini, R. Cancedda, F. Descalzi, M. Mastrogiacomo, *Tissue Eng., Part A* **2011**, *17*, 1787.

[21] F. Picard, B. Hersant, R. Bosc, J. P. Meningaud, *Wound Repair Regen.* **2015**, *23*, 163.

[22] W. J. Berghoff, W. S. Pietrzak, R. D. Rhodes, *Orthopedics* **2006**, *29*, 590.

[23] G. Filardo, E. Kon, A. Roffi, B. Di Matteo, M. L. Merli, M. Marcacci, *Knee Surg. Sports Traumatol. Arthrosc.* **2015**, *23*, 2459.

[24] M. J. Gardner, D. Demetrakopoulos, P. R. Klepchick, P. A. Mooar, *Int. Orthop.* **2007**, *31*, 309.

[25] R. A. Mlynarek, A. W. Kuhn, A. Bedi, *Am. J. Orthop.* **2016**, *45*, 290.

[26] A. M. Haleem, A. A. El Singergy, D. Sabry, H. M. Atta, L. A. Rashed, C. R. Chu, M. T. El Shewy, A. Azzam, M. T. A. Aziz, *Cartilage* **2010**, *1*, 253.

[27] T. Burnouf, D. Strunk, M. B. C. Koh, K. Schallmoser, *Biomaterials* **2016**, *76*, 371.

[28] R. Z. Lin, Y. C. Chen, R. Moreno-Luna, A. Khademhosseini, J. M. Melero-Martin, *Biomaterials* **2013**, *34*, 6785.

[29] J. W. Nichol, S. T. Koshy, H. Bae, C. M. Hwang, S. Yamanlar, A. Khademhosseini, *Biomaterials* **2010**, *31*, 5536.

[30] V. E. Santo, P. Babo, M. Amador, C. Correia, B. Cunha, D. F. Coutinho, N. M. Neves, J. F. Mano, R. L. Reis, M. E. Gomes, *Biomacromolecules* **2016**, *17*, 1985.

[31] K. Yue, X. Li, K. Schrobback, A. Sheikhi, N. Annabi, J. Leijten, W. Zhang, Y. S. Zhang, D. W. Hutmacher, T. J. Klein, et al., *Biomaterials* **2017**, *139*, 163.

[32] N. Annabi, S. M. Mithieus, P. Zorlutuna, G. Camci-Unal, A. S. Weiss, A. Khademhosseini, *Biomaterials* **2013**, *34*, 5496.

[33] V. Pavlovic, M. Ciric, V. Jovanovic, P. Stojanovic, *Open Med.* **2016**, *11*, 242.

[34] S. R. Caliari, J. A. Burdick, *Nat. Methods* **2016**, *13*, 405.

[35] C. A. Custódio, R. L. Reis, J. F. Mano, *Biomacromolecules* **2016**, *17*, 1602.

[36] M. C. Lampi, M. Guvendiren, J. A. Burdick, C. A. Reinhart-king, *ACS Biomater. Sci. Eng.* **2017**, *3*, 3007.

[37] A. D. Arya, P. M. Hallur, A. G. Karkisaval, A. Gudipati, S. Rajendiran, V. Dhavale, B.

Ramachandran, A. Jayaprakash, N. Gundiah, A. Chaubey, *ACS Appl. Mater. Interfaces* **2016**, *8*, 22005.

[38] O. Chaudhuri, L. Gu, M. Darnell, D. Klumpers, S. A. Bencherif, J. C. Weaver, N. Huebsch, D. J. Mooney, *Nat. Commun.* **2015**, *6*, 1.

[39] M. Marcinczyk, H. Elmashhady, M. Talovic, A. Dunn, F. Bugis, K. Garg, *Biomaterials* **2017**, *141*, 233.

[40] E. Chung, J. A. Rytlewski, A. G. Merchant, K. S. Dhada, E. W. Lewis, L. J. Suggs, *Acta Biomater.* **2015**, *17*, 78.

[41] T. Burnouf, H. A. Goubran, T.-M. Chen, K.-L. Ou, M. El-Ekiaby, M. Radosevic, *Blood Rev.* **2013**, *27*, 77.

[42] G. Walenda, H. Hemeda, R. K. Schneider, R. Merkel, B. Hoffmann, W. Wagner, *Tissue Eng., Part C* **2012**, *18*, 924.

[43] R. A. Marklein, J. A. Burdick, *Soft Matter* **2010**, *6*, 136.

[44] S. Khetan, J. A. Burdick, *Soft Matter* **2011**, *7*, 830.

[45] M. B. Oliveira, C. A. Custódio, L. Gasperini, R. L. Reis, J. F. Mano, *Acta Biomater.* **2016**, *41*, 119.

[46] A. Banerjee, M. Arha, S. Choudhary, R. S. Ashton, S. R. Bhatia, D. V. Schaffer, R. S. Kane, *Biomaterials* **2009**, *30*, 4695.

[47] A. J. Engler, S. Sen, H. L. Sweeney, D. E. Discher, *Cell* **2006**, *126*, 677.

[48] W. J. Hadden, J. L. Young, A. W. Holle, M. L. McFetridge, D. Y. Kim, P. Wijesinghe, H. Taylor-Weiner, J. H. Wen, A. R. Lee, K. Bieback, et al., *Proc. Natl. Acad. Sci. U.S.A.* **2017**, *114*, 5647.

[49] S. Even-Ram, V. Artym, K. M. Yamada, *Cell* **2006**, *126*, 645.

[50] A. I. Neto, P. A. Levkin, J. F. Mano, *Mater. Horiz.* **2018**, *5*, 379.

[51] V. E. Santo, A. R. C. Duarte, E. G. Popa, M. E. Gomes, J. F. Mano, R. L. Reis, *J. Controlled Release* **2012**, *162*, 19.

[52] P. S. Babo, X. Cai, A. S. Plachokova, R. L. Reis, J. A. Jansen, M. E. Gomes, X. F. Walboomers, *Tissue Eng., Part A* **2016**, *22*, 1164.

[53] R. Ito, N. Morimoto, L. H. Pham, T. Taira, K. Kawai, S. Suzuki, *Tissue Eng., Part A* **2013**, *19*, 1.

The table of contents entry should be 50–60 words long, and the first phrase should be bold. The entry should be written in the present tense and impersonal style. The text should be different from the abstract text.

Keyword

C. Author 2, D. E. F. Author 3, A. B. Corresponding Author* ((same order as byline))

Title: Photopolymerizable platelet lysates hydrogels for customizable 3D cell culture platforms

ToC figure ((Please choose one size: 55 mm broad × 50 mm high **or** 110 mm broad × 20 mm high. Please do not use any other dimensions))

ToC

Figure 1

Click here to access/download

Production Data

Figure 1.tif

Figure 2

Figure 3

Click here to access/download

Production Data

Figure 3.tif

Figure 4

Figure 5

Figure 6

Figure 7

Figure 8

Figure 9

Figure 10


Click here to access/download
Production Data
Figure 10.tif